

Photocatalytic CO₂ Reduction Using Cu(I) Photosensitizers with a Fe(II) CatalystHiroyuki Takeda,[†] Kenji Ohashi,[†] Akiko Sekine,[‡] and Osamu Ishitani^{*,†}[†]Department of Chemistry, Graduate School of Science and Engineering, Tokyo Institute of Technology, 2-12-1-NE-1 O-okayama, Meguro-ku, Tokyo 152-8550, Japan[‡]Department of Chemistry and Material Science, Graduate School of Science and Engineering, Tokyo Institute of Technology, 2-12-1-H60 O-okayama, Meguro-ku, Tokyo 152-8551, Japan

Supporting Information

ABSTRACT: Photocatalytic systems developed from complexes with only abundant metals, i.e., Cu^I(dmp)(P)₂⁺ (dmp = 2,9-dimethyl-1,10-phenanthroline; P = phosphine ligand) as a redox photosensitizer and Fe^{II}(dmp)₂(NCS)₂ as a catalyst, produced CO as the main product by visible light irradiation. The best photocatalysis was obtained using a Cu^I complex with a tetradentate dmp ligand tethering two phosphine groups, where the turnover number and quantum yield of CO formation were 273 and 6.7%, respectively.

Photocatalytic CO₂ reduction is one of the most important reactions in artificial photosynthesis research and is expected to become a key technology for addressing global warming and shortage of energy and carbon resources.¹ Metal polypyridine complexes are often used as a main component, i.e., a redox photosensitizer (PS) and/or a catalyst (CAT), in various photocatalytic systems for CO₂ reduction.² In most studies, complexes with expensive and rare metal ions, e.g., Ru^{II} and Re^I, have been used as the PS and/or CAT because of their fascinating photochemical and/or electrochemical properties.³ Recently, Ir^{III} complexes as a PS or as a photocatalyst have been applied in the photocatalytic reduction of CO₂.⁴ However, photocatalytic systems using only abundant elements need to be developed because considerable CO₂ is expected to be utilized in the future. Although a limited number of complexes with more abundant metals, i.e., Co^I and Ni^I macrocycles, Fe^{II} porphyrins, and Co^{II} and Mn^I diimine complexes, were reported as CATs in the photocatalytic reduction of CO₂, rare metal complexes, i.e., Ru and Ir complexes, were used as PSs.^{4b-d,5} A Fe^{III} porphyrin was successfully used as a photocatalyst for the reduction of CO₂ to CO,⁶ however, the durability of the CAT was low (TON_{CO} = ~30).^{6b} Although mixed systems of Fe^{III} porphyrin as a CAT with 9-cyanoanthracene as an organic PS showed better durability (TON_{CO} = ~60), the quantum yield of CO formation was very low (8 × 10⁻⁴ %).^{4c}

Herein, we report a novel, efficient, and durable CO₂-reduction photocatalytic system using only nonprecious metal complexes, i.e., Cu^I diimine complexes as the PS and a Fe^{II} diimine complex as the CAT (Figure 1).

As the PS, we chose heteroleptic Cu^I complexes with both diimine and phosphine ligands, as shown in Figure 1a because

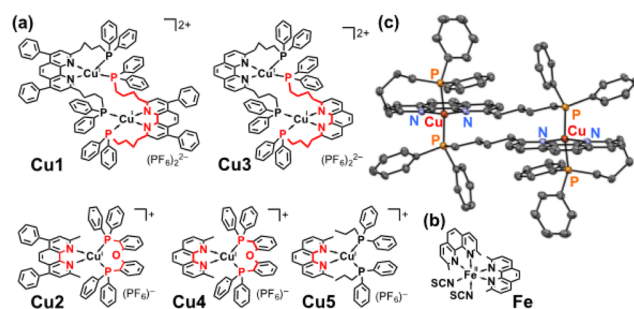


Figure 1. Structures of the Cu^I PSs (a) and the Fe^{II} CAT (b) and an ORTEP drawing of Cu₃ (c). Displacement ellipsoids are shown at the 50% probability level. Hydrogen atoms, PF₆⁻ anions, and solvent molecules were omitted in (c) for clarity.

of their longer lifetimes (>10 μs)⁷ and stronger oxidation power in the excited state compared with homoleptic Cu^I(N[^]N)₂⁺-type complexes (N[^]N = diimine ligand); Cu^I and Cu₃ were newly synthesized using tetradentate ligands, where the two phosphine ligands are tethered to the 2,9-positions of phenanthroline (phen) and bathophenanthroline (baphen) with propyl chains (abbreviated as P₂phen and P₂baphen, respectively). X-ray single-crystal analysis of Cu₃ (Figure 1c) showed that two Cu^I complexes dimerized with two P₂phen molecules as bridging ligands, each supplying the bidentate phen moiety and one monodentate phosphine moiety to one Cu^I center and another phosphine moiety to another Cu^I center. Each Cu^I complex unit had a tetrahedral structure, which is similar to that of the corresponding mononuclear complex, i.e., Cu^I5 (Figure S1b). Variable-temperature (VT) ¹H NMR analyses of the phenylphosphine groups in Cu₃ (Figures S2–S7) indicated that two types of phosphine moieties exchanged with each other in CD₃CN solution, even at 22 °C (*k*_{ex} = 40 s⁻¹, Δ*G*[‡] = 15 kJ mol⁻¹). Because this phenomenon can be simulated by assuming only a simple exchange between the corresponding proton peaks, the dimeric structure of Cu₃ should be maintained in solution, even at temperatures between -44 and 75 °C. Similar phenomena were observed in the VT-NMR spectrum of Cu^I (50 s⁻¹ at 22 °C, Δ*G*[‡] = 15 kJ mol⁻¹). This clearly indicates

Received: February 22, 2016

Published: March 25, 2016

that **Cu1** has dimeric structure to similar to that of **Cu3** in solution.

In the photocatalytic reactions, the concentrations of the binuclear Cu complexes (**Cu1** and **Cu3**) were half those of the mononuclear complexes (**Cu2**, **Cu4**, and **Cu5**), i.e., 0.25 and 0.5 mM, respectively. As a sacrificial reductant, 1,3-dimethyl-2-phenyl-2,3-dihydro-1H-benzo[d]imidazole (BIH)⁸ was used; this compound efficiently quenched the excited states of the Cu complexes, as shown below. Fe^{II}(dmp)₂(NCS)₂ (**Fe**, Figure 1b)⁹ was used as the CAT in the photocatalytic reactions for two reasons: this complex had electrocatalytic ability toward CO₂ reduction at $>E = -1.5$ V vs Ag/AgNO₃, which was indicated by its cyclic voltammogram (CV) measured in CH₃CN-triethanolamine (TEOA) (5:1 v/v) under a CO₂ atmosphere (Figure S8), and the complex had relatively weak absorption in the visible region (Figure S9).

In a typical photocatalytic reaction, a CH₃CN-TEOA (5:1 v/v) mixed solution (4 mL) containing **Cu1** (0.25 mM), **Fe** (0.05 mM), and BIH (10 mM) was irradiated using 436 nm monochromatic light, giving CO as the main product with H₂ but almost no HCOOH (Figure S10); the turnover number (TON^{CAT}) based on the used **Fe** reached 95 (19.0 μmol) for CO and 56 (11.1 μmol) for H₂ after 5 h irradiation, and the selectivity of the CO formation was 70.5%. Note that more than 75% of the added BIH should already be consumed during the irradiation because CO and H₂ are two-electron-reduced products of CO₂ and protons, respectively, and BIH is a two-electron donor.⁸ Accordingly, BIH concentration in the reaction solution was increased to 50 mM. After 12 h irradiation, 54.5 μmol of CO (TON^{CAT}_{CO} = 273) and 15.0 μmol of H₂ (TON^{CAT}_{H₂} = 75) were produced; the selectivity of CO formation was 78%. Note that almost all of the added **Cu1** remained in the reaction solution even after the irradiation (Figure S11). Thus, **Cu1** is a tremendously stable redox PS.

A control experiment without **Cu1** gave neither CO nor H₂. In the absence of **Fe**, on the other hand, **Cu1** photocatalyzed only H₂ evolution, giving 9.5 μmol H₂ with a very small amount of CO (0.3 μmol). Decomposition of **Cu1** in the photocatalytic reaction might give other catalysts for only H₂ evolution but not CO₂ reduction. Since, however, **Cu1** was very stable in the presence of the Fe catalyst in the photocatalytic reaction condition, the effects of the decomposition products of **Cu1** should not be so important for determining the product distribution. The carbon source of the produced CO was confirmed by a tracer experiment using ¹³CO₂ (99% of the ¹³C content). The produced ratio of ¹³CO to ¹²CO was 99:1 (Figure S12), indicating that CO was produced by the reduction of CO₂. These results clearly show that the photocatalytic CO₂ reduction requires both **Cu1** as the PS and **Fe** as the CAT, and the **Cu1**-**Fe** system can photocatalyze CO₂ reduction with high efficiency. The formation quantum yields (Φ) of CO and H₂ were 6.7% and 2.8%, respectively. This efficiency is the highest among the reported photocatalytic systems using Fe complexes as the CAT. Note that the ratio of PS to CAT was 10:1 in this system; however, in many of the photocatalytic systems using abundant metal complexes as the CAT, the ratio of PS to CAT was much higher, i.e., 10,000:100; meanwhile, the TON based on the PS used was very low, even though TON^{CAT} was high.

Table 1 summarizes the results of the photocatalytic reactions, including systems using other Cu^I complexes as the PS instead of **Cu1** ([BIH] = 10 mM). Although another dimeric Cu complex, **Cu3**, with P₂phen ligands instead of

Table 1. Photocatalytic abilities of mixed systems with Cu^I PSs and Fe^{II} CAT

		Fe + PS			
		(0.05 mM)	(Dimeric Complex: 0.25 mM) (Monomeric Complex: 0.5 mM)	$h\nu$ (436 nm)	
CO ₂		BIH (10 mM) in CH ₃ CN / TEOA (5:1 v/v)			
		products ^b (μmol)		Φ ^c (%)	
PS	t ^a (h)	CO	H ₂	CO	H ₂
Cu1	1	14.6	9.0	6.7	2.8
	5	19.0	11.1		
Cu1 ^d	12	54.5	15.0		
Cu1 ^e	5	0.3	9.5		
none	5	n.d. ^f	n.d. ^f		
Cu2	1	11.1	7.6	2.6	2.0
	5	23.4	15.5		
Cu3	1	6.1	5.6	2.3	1.1
	5	13.4	9.0		
Cu4	1	5.9	4.8	1.1	0.6
	5	13.9	11.7		
Cu5	5	n.d. ^f	n.d. ^f		

^aIrradiation time. ^bA high-pressure Hg lamp ($\lambda_{\text{ex}} = 435.8$ nm, see Experimental Details in SI) was used. ^cQuantum yield as a ratio of the number of the product molecules and absorbed photons (Figure S13). A Xe lamp was used with a band-pass filter ($\lambda_{\text{ex}} = 436 \pm 5$ nm, light intensity: 5×10^{-8} einstein s⁻¹, see Experimental Details in SI). ^dConcentration of BIH was 50 mM. ^eIn the absence of **Fe**. ^fNot detected.

P₂baphen, could also be used as the PS, the efficiency was lower than that obtained using **Cu1**. In the three photocatalytic systems using the monomeric Cu complexes, **Cu2** showed the highest TON_{CO}, which was similar to the system using the dimer **Cu1**. However, Φ_{CO} (2.6%) was much lower compared to the system using **Cu1**. The photocatalytic ability for CO₂ reduction using **Cu4**, which contains a 2,9-dimethyl-phen ligand, was much lower than that using **Cu2**, which contains the 2,9-dimethyl-baphen ligand (Figure S13). Interestingly, the system using **Cu5** as the PS showed photocatalytic ability for neither CO₂ reduction nor H₂ evolution; the reason for this is discussed later. The comparison between the photocatalytic activities of these systems clearly shows that the introduction of either phenyl groups or two phosphine units into the phen ligand enhanced the ability of the Cu complex as a PS.

To clarify the reason(s) behind this result, we investigated the photophysical, electrochemical, and photochemical properties of the Cu complexes in detail (Tables S3 and S4). UV-vis absorption spectra of all Cu^I complexes (Figure S14) showed a broad band at 350–450 nm, attributable to singlet metal-to-ligand charge transfer (¹MLCT) excitation. The spectra of **Cu2** and **Cu5** only contained a small shoulder, which was not observed in that of CH₂Cl₂, at around 450–500 nm due to a partial ligand exchange proceeding even in the dark to produce the corresponding homoleptic Cu^I(N[^]N)₂⁺ complexes.¹⁰ On the other hand, spectral characteristics due to the ligand exchange were not observed in the cases of Cu^I complexes having the tetradentate ligand, i.e., **Cu1** and **Cu3**.

In CH₂Cl₂, all Cu^I complexes showed broad emissions at 450–800 nm with high quantum yields (Φ_{em} = 0.17–0.52) and long lifetimes (τ_{em} = 11.0–19.4 μs), even at room temperature. It has been reported that emission from Cu^I diimine complexes can be attributed to delayed fluorescence from their ¹MLCT excited states and is significantly quenched in solvent; this is

because solvent molecules can coordinate to metal ions following flattening of the tetrahedral structures of the Cu complexes.¹¹ In CH₃CN, emission from the Cu^I complexes (Figure S14) was partially quenched in the cases of Cu1–Cu4 and completely quenched in the case of Cu5; however, the emissive properties of Cu1 and Cu3 were relatively well preserved, with τ_{em} of $\sim 4 \mu s$ and Φ_{em} of ~ 0.04 , compared with those of Cu2 and Cu4 ($\tau_{em} \sim 1 \mu s$ and $\Phi_{em} \sim 0.03$) (Figure S16 and Table S3). The lack of photocatalysis of the system using Cu5 is likely due to the short lifetime of the excited Cu5 in CH₃CN. Reductive quenching of the excited states of Cu1–Cu4 by BIH was investigated by Stern–Volmer experiments (Figures S16–20); linear relationships were observed between BIH concentration and both I_0/I and τ_0/τ , and these two plots overlapped each other in all cases. This clearly indicates that the quenching of emission from the Cu complexes by BIH was a dynamic process. The excited-state quenching rates (k_q^{BIH}) of the Cu^I complexes by BIH were $2.2\text{--}5.6 \times 10^9 \text{ M}^{-1} \text{ s}^{-1}$ (Table S4), and most of the excited Cu1–Cu4 complexes were quenched by 10 mM of BIH (the quenching fractions, η_q^{BIH} , were 95–97%). On the other hand, quenching by Fe, CO₂, or TEOA, which is required as a base for removing a proton from the one-electron-oxidized species of BIH, was not observed under the photocatalytic reaction conditions.

UV–vis absorption spectral changes in CH₃CN–TEOA (5:1 v/v) solutions containing Cu1 or Cu2 were observed during irradiation in the presence of BIH (10 mM) under an Ar atmosphere (Figure S21a,d). Just after the irradiation began, a new broadband arose around 700 nm, which is attributable to the one-electron-reduced species (OERS) of the Cu complex because a similar absorption was observed in controlled electrolysis of the Cu^I complexes at $-2.0 \text{ V vs Ag/AgNO}_3$ (Figure S21b,e; CVs of Cu1 and Cu2 are shown in Figure S25). The OERSs accumulated immediately after starting the irradiation and then reached the maximum amounts (Figures S21c,f). Although further irradiation caused a decrease in the OERSs, this decrease was much slower in the case of Cu1 than Cu2. In the cases of Cu3 and Cu4, on the other hand, the OERSs were not observed even in the first stage of irradiation (Figure S22). These results suggest that the higher stability of the OERS of Cu1 induced more efficient capability as a PS.

The stability of the OERS of Cu1 was also confirmed by its CV (Figure S25); a reversible one-electron reduction wave was observed at $E_{1/2} = -1.95 \text{ V vs Ag/AgNO}_3$. Although the first reduction wave in the CV of Cu2 was also reversible ($E_{1/2} = -1.96 \text{ V}$), the reversibility of the first reduction waves of Cu3, Cu4, and Cu5 ($E_{1/2} = -2.01, -2.03, \text{ and } -1.98 \text{ V}$, respectively) was clearly lower, and the reverse scan to the positive potential after the cathodic scan gave an additional sharp peak or peaks at -0.20 and -0.55 V in the case of Cu4 and at -0.60 V in the case of Cu5.

The first reduction wave of Fe, which was measured in CH₃CN–TEOA (5:1 v/v) under a CO₂ atmosphere, was observed at $E_p = -1.61 \text{ V}$, followed by a catalytic wave, with an onset potential of -1.8 V (Figure S8). This clearly indicates that both first and second reductions of Fe by the OERS of all Cu complexes are thermodynamically favorable processes. Actually, under the photocatalytic reaction conditions in the presence of both CO₂ and Fe, accumulation of the OERSs of the Cu complexes could not be observed, even in the experiments using Cu1 and Cu2 (Figures S21c,f, S23, and S24).

In conclusion, we successfully constructed an efficient and durable photocatalytic system for CO₂ reduction using

abundant metal complexes, i.e., Cu1 as the PS and Fe as the CAT. The abilities of the Cu^I complexes can be improved by the introduction of both a tetradentate ligand and phenyl groups into the 4,7-position of the phen moiety of the tetradentate ligand. The photocatalytic reduction of CO₂ proceeded via (1) reductive quenching of the excited Cu PS with BIH and (2) first and second electron transfer processes from the OERS of the Cu PS to the Fe CAT. A more detailed mechanistic study of CO₂ reduction, especially CO₂ reduction processes on the Fe CAT, is underway in our laboratory.

■ ASSOCIATED CONTENT

Supporting Information

The Supporting Information is available free of charge on the ACS Publications website at DOI: 10.1021/jacs.6b01970.

Crystallographic data (CIF)

Experimental details and data (PDF)

■ AUTHOR INFORMATION

Corresponding Author

*ishitani@chem.titech.ac.jp

Notes

The authors declare no competing financial interest.

■ ACKNOWLEDGMENTS

This work was supported by CREST, JST.

■ REFERENCES

- (1) Concepcion, J. J.; House, R. L.; Papanikolas, J. M.; Meyer, T. J. *Proc. Natl. Acad. Sci. U. S. A.* **2012**, *109*, 15560–15564.
- (2) (a) Fujita, E. *Coord. Chem. Rev.* **1999**, *185–186*, 373–384. (b) Yamazaki, Y.; Takeda, H.; Ishitani, O. *J. Photochem. Photobiol., C* **2015**, *25*, 106–137.
- (3) (a) Ishida, H.; Terada, T.; Tanaka, K.; Tanaka, T. *Inorg. Chem.* **1990**, *29*, 905–911. (b) Kuramochi, Y.; Itabashi, J.; Fukaya, K.; Enomoto, A.; Yoshida, M.; Ishida, H. *Chem. Sci.* **2015**, *6*, 3063–3074. (c) Hawecker, J.; Lehn, J.-M.; Ziessel, R. *Helv. Chim. Acta* **1986**, *69*, 1990–2012. (d) Morimoto, T.; Nishiura, C.; Tanaka, M.; Rohacova, J.; Nakagawa, Y.; Funada, Y.; Koike, K.; Yamamoto, Y.; Shishido, S.; Kojima, T.; Saeki, T.; Ozeki, T.; Ishitani, O. *J. Am. Chem. Soc.* **2013**, *135*, 13266–13269. (e) Tamaki, Y.; Koike, K.; Morimoto, T.; Yamazaki, Y.; Ishitani, O. *Inorg. Chem.* **2013**, *52*, 11902–11909.
- (4) (a) Sato, S.; Morikawa, T.; Kajino, T.; Ishitani, O. *Angew. Chem., Int. Ed.* **2013**, *52*, 988–992. (b) Thoi, V. S.; Kornienko, N.; Margarit, C. G.; Yang, P.; Chang, C. J. *J. Am. Chem. Soc.* **2013**, *135*, 14413–14424. (c) Bonin, J.; Robert, M.; Routier, M. *J. Am. Chem. Soc.* **2014**, *136*, 16768–16771. (d) Chen, L.; Guo, Z.; Wei, X.-G.; Gallenkamp, C.; Bonin, J.; Anxolabehère-Mallart, E.; Lau, K.-C.; Lau, T.-C.; Robert, M. *J. Am. Chem. Soc.* **2015**, *137*, 10918–10921.
- (5) (a) Tinnemans, A. H. A.; Koster, T. P. M.; Thewissen, D. H. M. W.; Mackor, A. *Recl. Trav. Chim. Pays-Bas* **1984**, *103*, 288–295. (b) Ziessel, R.; Hawecker, J.; Lehn, J.-M. *Helv. Chim. Acta* **1986**, *69*, 1065–1084. (c) Takeda, H.; Koizumi, H.; Okamoto, K.; Ishitani, O. *Chem. Commun.* **2014**, *50*, 1491–1493. (d) Fei, H.; Sampson, M. D.; Lee, Y.; Kubiak, C. P.; Cohen, S. M. *Inorg. Chem.* **2015**, *54*, 6821–6828.
- (6) (a) Grodkowski, J.; Behar, D.; Neta, P.; Hambright, P. *J. Phys. Chem. A* **1997**, *101*, 248–254. (b) Bonin, J.; Chaussemier, M.; Robert, M.; Routier, M. *ChemCatChem* **2014**, *6*, 3200–3207.
- (7) (a) Cutteli, D. G.; Kuang, S.-M.; Fanwick, P. E.; McMillin, D. R.; Walton, R. A. *J. Am. Chem. Soc.* **2002**, *124*, 6–7. (b) Luo, S.; Mejia, E.; Friedrich, A.; Pazidis, A.; Junge, H.; Surkus, A.-E.; Jackstell, R.; Denurra, S.; Gladiali, S.; Lochbrunner, S.; Beller, M. *Angew. Chem., Int. Ed.* **2013**, *52*, 419–423. (c) Lazorski, M. S.; Castellano, F. N. *Polyhedron* **2014**, *33*, 57–70. (d) Tsubomura, T.; Kimura, K.

- Nishikawa, M.; Tsukuda, T. *Dalton Trans.* **2015**, *44*, 7554–7562.
- (e) Saito, K.; Arai, T.; Takahashi, N.; Tsukuda, T.; Tsubomura, T. *Dalton Trans.* **2006**, 4444–4448.
- (8) Tamaki, Y.; Koike, K.; Morimoto, T.; Ishitani, O. *J. Catal.* **2013**, *304*, 22–28.
- (9) König, E.; Ritter, G.; Madeja, K. *J. Inorg. Nucl. Chem.* **1981**, *43*, 2273–2280.
- (10) Kaeser, A.; Mohankumar, M.; Mohanraj, J.; Monti, F.; Holler, M.; Cid, J.-J.; Moudam, O.; Nierengarten, I.; Karmazin-Brelot, L.; Duhayon, C.; Delavaux-Nicot, B.; Armaroli, N.; Nierengarten, J.-F.; Duhayon, C.; Coppel, Y.; Nierengarten, J.-F. *Inorg. Chem.* **2013**, *52*, 12140–12151.
- (11) McMillin, D. R.; Kirchoff, J. R.; Goodwin, K. V. *Coord. Chem. Rev.* **1985**, *64*, 83–92.